Available online at www.sciencedirect.com

ScienceDirect

Procedia CIRP 126 (2024) 372–377

www.elsevier.com/locate/procedia

17th CIRP Conference on Intelligent Computation in Manufacturing Engineering (CIRP ICME '23)

Improving dynamic process stability in finishing of thin-walled workpieces by optimal selection of stock shape

Pascal Kienast[a,*], L. Taner Tunç[b], Recep Koca[c], Ozan Ölgü[c], Philipp Ganser[a], Thomas Bergs[a,d]

[a]*Fraunhofer Institute for Production Technology IPT, Steinbachstr. 17, 52074 Aachen, Germany*
[b]*Manufacturing Research Lab, Faculty of Engineering and Natural Sciences, Sabanci University, 34956 Istanbul, Türkiye*
[c]*TUSAS Engine Industries Inc. (TEI), 26210 Eskişehir, Türkiye*
[d]*Laboratory for Machine Tools and Production Engineering (WZL), RWTH Aachen University, Campus-Boulevard 30, 52074 Aachen, Germany*
*Corresponding author. Tel.: +49-241-8904-330. *E-mail address:* pascal.kienast@ipt.fraunhofer.de

Abstract

In 5-axis milling of thin-wall parts, flexibility of the in-process-workpiece (IPW) governs static and dynamic deflections, especially at the semi-finishing and finishing stages. Thus, the near net shape preform, i.e. the stock shape left for semi/finishing is crucial for chatter stability. In this study, a methodology is presented to design the stock shape for improved stability. Coupled process simulation, which includes material removal, finite element analysis (FEA) and process stability simulations, is used to show the effect of stock shape on chatter stability. Spindle speed is optimized along the toolpath based on the varying process dynamic behavior for selected cutter locations (CL). The proposed method is experimentally demonstrated on case studies.

© 2024 The Authors. Published by Elsevier B.V.
This is an open access article under the CC BY-NC-ND license (https://creativecommons.org/licenses/by-nc-nd/4.0)
Peer-review under responsibility of the scientific committee of the 17th CIRP Conference on Intelligent Computation in Manufacturing Engineering (CIRP ICME'23)

Keywords: milling; 5-axis; process stability; chatter; vibration, in-process workpiece, machining strategy, coupled process simulation

1. Introduction

Chatter vibrations in milling processes leads to workpiece damages, premature tool wear and many more unfavorable effects [1]. Thin-walled features such as aero engine blades are subject to chatter, especially in the semi-finish and finish milling phases, as they become more and more flexible due to material removal [2]. Milling of thin-wall geometries can be considered as one of the most complex machining processes, where selecting high performance, chatter-free milling parameters is challenging [3]. Thus, usually conservative values of feed rate and depth of cut are selected, hindering process productivity.

In order to achieve chatter-free high performance milling, specifically, the workpiece and tool dynamics are required to be known for stability analysis at the cutting zone [4]. For this purpose, identification of the frequency response function (FRF) of tool and workpiece is essential [5]. However, the FRF of the workpiece is not only position-dependent due to local workpiece mode shapes [6], but also varies continuously due to material removal [7] and hence stability lobes. Thus, selecting constant spindle speed can lead to local chatter areas on the workpiece surface. Spindle speed variation in machining [8,9] is known to be one of the techniques to improve stability, which applicable on milling of thin-walled workpieces, as well. Another approach is adjusting the material removal sequence [10,11]. By designing the machining strategy, it is possible to control the underlying dynamic properties and thus affecting the efficiency and stability of the machining task [12].

In this paper, the proposed approach by Tunç et al. [13] to select the thickness and shape of the stock for improved stability in 5-axis milling of thin-wall workpieces is further

2212-8271 © 2024 The Authors. Published by Elsevier B.V.
This is an open access article under the CC BY-NC-ND license (https://creativecommons.org/licenses/by-nc-nd/4.0)
Peer-review under responsibility of the scientific committee of the 17th CIRP Conference on Intelligent Computation in Manufacturing Engineering (CIRP ICME'23)
10.1016/j.procir.2024.08.378

elaborated for an application-oriented use case. Here, the stock thickness and shape are decided considering in-process-workpiece (IPW) dynamics using finite element analysis (FEA).

Henceforth, the workpiece demonstrator with its reference process and variable stock shape cases are given in Section 2. The workflow of coupled technology models used in process simulation are presented in Section 3. Section 4 discusses the effect of stock shape on the FRF of the IPW and hence stability diagrams, through case studies. An experimental demonstration is given in Section 5, where three selected cases are applied. Conclusions are derived and an outlook is discussed in Section 6.

2. Definition of workpiece, reference process and cases

Section 2.1 initially introduces the workpiece demonstrator, simplified from a blisk with 36 blades to a single blade. Subsequently, Section 2.2 presents the programmed machining operations for the reference process. In Section 2.3, the consideration of constraints and the definition of simulation cases with different variable stock shapes are described.

2.1. Workpiece demonstrator

The demonstrator geometry is simplified from a complete blisk having 36 blades (Fig. 1a) to a single blade (Fig. 1b), made of Ti-6Al-4V. However, all the constraints and aspects of full blisk milling are considered. The nominal geometry of the blade has a profile height of 60 mm and chord length of 40 mm. The blade thickness varies from a minimal thickness of 0.5 mm to a maximum thickness of 1.5 mm.

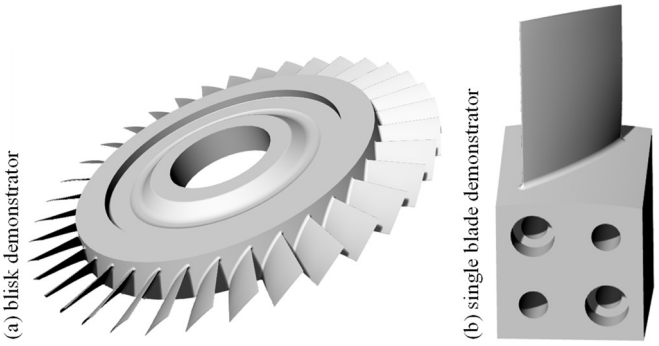

Fig. 1. Workpiece demonstrator.

2.2. Reference process setup

The milling strategy consists of a multi-stage process including: (i) pre-roughing process (Fig. 2a), with the aim of cutting the material with a high removal rate, (ii) modified roughing process (Fig. 2b) to generate the variable stock shape for the subsequent process, and (iii) merged semi-/finishing processes (Fig. 2c) to produce the required geometrical accuracy. Here, the processes are examined for the entire blade – from shroud to hub. It is noteworthy to emphasized that, in the merged semi-finish/finish milling process, as very small stock thickness is left to the finishing, any chatter vibration occurring in the semi-finishing process directly leaves deep marks for the finishing process, which cannot be removed.

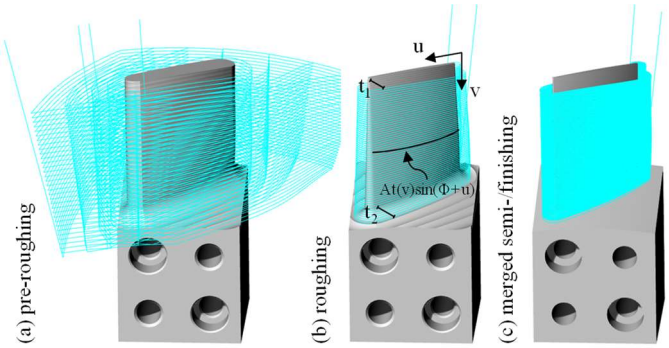

Fig. 2. Machining operations.

The thickness of the tapered stock, remaining after (ii), increases from a minimal thickness of 0.25 mm at the shroud to a maximum thickness of 2.5 mm at the hub (case 0 in Table 1). Consequently, the radial depth of cut, respectively the blade material offset, varies between a_e = 0.20 mm at the shroud and a_e = 2.45 mm at the hub for semi-finishing. Axial depth of cut was set to a_p = 1 mm and the feed per tooth was defined as f_z = 0.06 mm. For finishing, the axial depth of cut was set to a_p = 0.25 mm, the radial depth of cut was set to a_e = 0.05 mm, and the feed per tooth was defined as f_z = 0.06 mm.

2.3. Constraints and case study

Twelve cases are determined to compare the effect of stock shape as given in Table 1, subject to the constraint of the minimum distance of 16.3 mm, between two adjacent blades for the blisk demonstrator (Fig. 1a). To design productive roughing process, the tool diameter is not selected smaller than 10 mm, which results in a maximum thickness at the blade hub of 3 mm. The thickness distribution parameters are as follows: t_1, t_2 is the thickness at the blade shroud, respectively the hub, A is the amplitude variation, and Φ is the phase shift of the sinusoidal variation from leading to trailing edge (see Fig. 2b).

Table 1. Thickness distribution parameters for the case study.

Case	Type u / v	t_1 [mm]	t_2 [mm]	t_1/t_2	A [%]	Φ [deg]
0	const./lin.	0.25	2.5	10	-/-	-/-
1	const./lin.	0.50	2.5	20	-/-	-/-
2	const./lin.	0.75	2.5	30	-/-	-/-
3	const./lin.	1.00	2.5	40	-/-	-/-
4	const./lin.	0.30	3.0	10	-/-	-/-
5	const./lin.	0.60	3.0	20	-/-	-/-
6	const./lin.	0.90	3.0	30	-/-	-/-
7	const./lin.	1.20	3.0	40	-/-	-/-
8	sine/lin.	0.25	2.5	10	10	0
9	sine/lin.	0.25	2.5	10	30	0
10	sine/lin.	0.25	2.5	10	50	0
11	sine / lin.	0.25	2.5	10	30	90

Case 0 is used as reference, case 2 to case 7 involve variation along v-direction (leading to trailing edge), and case 8 to case 11 involve variation along u- (shroud to hub) and v-directions. The modification of the initially programmed toolpath was performed as described in [13].

3. Process simulation with coupled technology models

This section presents the workflow of FEA-coupled process simulations. Section 3.1 presents the systematic selection of cutter locations (CL) in the CAM system and the generation of corresponding IPWs. Subsequently, Section 3.2 deals with the automated FE modal analysis. In Section 3.3, the applied stability calculation is described.

3.1. Systematic CL selection and automated IPW generation

Based on the programmed toolpath, CLs were selected as proposed by Rudel and Kienast et al. in [14]. In this study, three vertical and six horizontal curves, i.e., cutter location layer (CLL), formed the grid on suction and pressure side of the blade and an offset of 2 mm to the blade edges was defined. IPWs were automatically generated after semi-finishing path number 6, 11, 21, 31, 41, 51 to capture the continuously changing workpiece dynamics (Fig. 33). Note that CL 4 to 6 are located on the pressure side as shown in Fig. 3e.

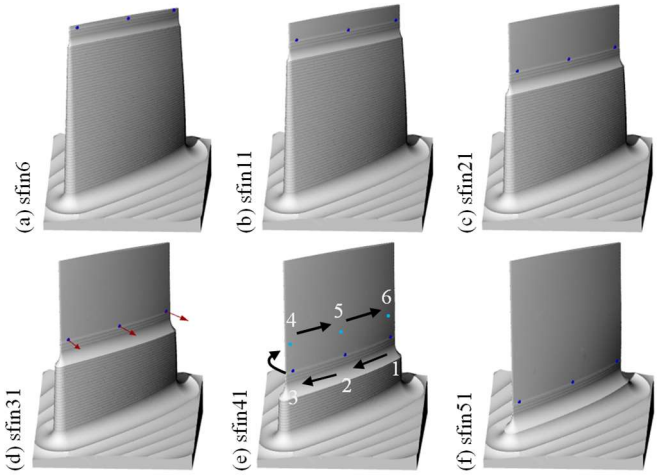

Fig. 3. Selection of cutter locations used for subsequent FE modal analysis.

3.2. Automated FE modal analysis

In the FE modal simulation, the material properties for Ti-6Al-4V were defined with Young's modulus of 119 GPa and density of 4436 kg/m^3. The element size was set to 0.8 mm to mesh the IPWs as recommended in [8,14]. A damping factor of 0.2 % was used in the numerical calculation of eigenmodes was set up to 12,000 Hz. The boundary conditions were defined in accordance with the machine setup shown in Fig. 11. Finally, the results of the blade dynamics at the corresponding CL in form of a state-space-model were exported from ANSYS. These steps were repeated for each CL, respectively each IPW.

The dynamics of the tool is determined using experimental modal analysis (EMA), where the modal parameters are shown in Table 2. In stability analysis, feed-direction is to be understood as y-direction, cross-feed is oriented in x-direction of the milling machine (see Fig. 11).

Table 2. Cutting conditions and modal parameters of the milling tool.

Cutting parameters					
Material	K_t, K_r [MPa]	Tool diameter	No. flutes	Mode	Radial [%]
TiAl6V4	2433, 677	12 mm	4	down	0.42 %

Modal parameters					
f [Hz]		ζ [%]		k [N/µm]	
x	y	x	y	x	y
1182, 1835, 2554	1191, 1889, 2585	3.6, 4.3, 6.3	2.9, 4.2, 4.1	12.5, 25.4, 34.3	14.1, 23.7, 50.2

3.3. Stability analysis

Subsequently, the modal parameters were further processed in a coupled stability analysis using zero order approximation (ZOA) [15]. Here, the simulated IPW FRF in x, y, and z directions (in workpiece coordinate system) are projected along the surface normal vector (see Fig. 3d), where the workpiece is assumed to be flexible and contributes to milling dynamics in the cross-feed direction. The stability lobe diagrams (SLD) are calculated for 2000 to 15000 RPM to cover the applicable spindle speed range for both semi-finishing and finishing. Radial depth, a_e, is considered variable for semi-finishing according to the variation of the stock thickness at the corresponding CL.

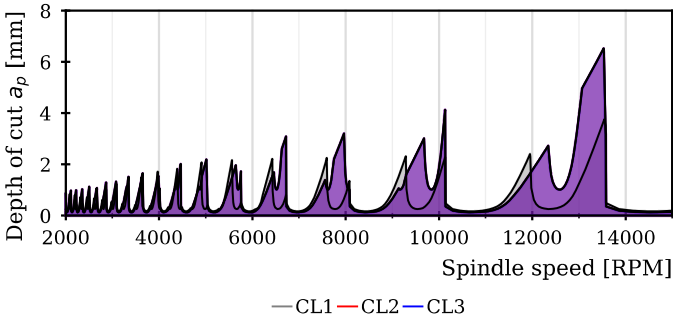

Fig. 4. SLD exemplary for finishing of case 0 "reference" before final merged semi-/finishing operation.

In Fig. 4, a representative SLDs are given for finishing of case 0 "reference" before final merged semi-/finishing operation for CL 1 to 3. It is seen that both the stability limits and the location of stability lobes significantly varies among the CLs (see Fig. 4), which constitutes the basis of variable stock selection (see Fig. 8).

4. Effect of stock shape on IPW dynamics and SLDs

Section 4.1 describes the effect of defined cases and therefore variable stock on IPW dynamics considering resultant FRF at CL 3 of IPW sfin6 (Fig. 3a). The further effect on process stability by analyzing stability lobe diagrams is demonstrated in Section 4.2. Finally, Section 4.3 introduces a novel approach for comprehensive evaluation of dynamic process stability.

4.1. Effect of variable stock on IPW FRF

In simulation of the IPW dynamics, constant damping ratio is used for all cases. In Fig. 5, the dynamic response of the workpiece is compared for four different cases. It is clearly seen that the amplitude of the 1st mode decreases with increasing thickness (case 0 to case 3) at the top section, i.e., shroud, of the blade. The 1st natural frequency (bending mode) tends to decrease, as well. The 2nd mode (torsional mode) is more affected in terms of the frequency shift. With the increased stock thickness, the frequency of the torsional mode increases and the dynamic amplitude decreases (Fig. 5).

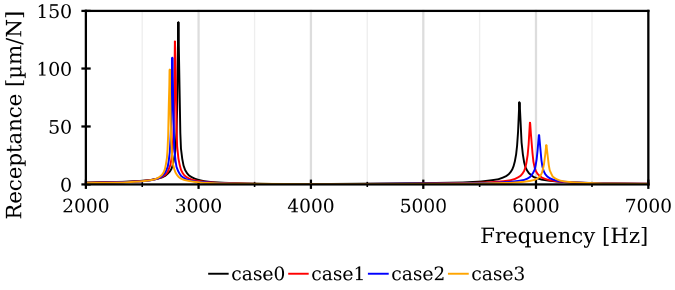

Fig. 5. Effect of increasing thickness at blade shroud on IPW FRFs.

By increasing the thickness at the root (case 0 vs. case 4), the first and second mode are significantly shifted to higher frequencies (see Fig. 6). The FRF amplitude is significantly reduced, a similar trend can be observed for increased thickness at blade shroud (case 4 to case 7).

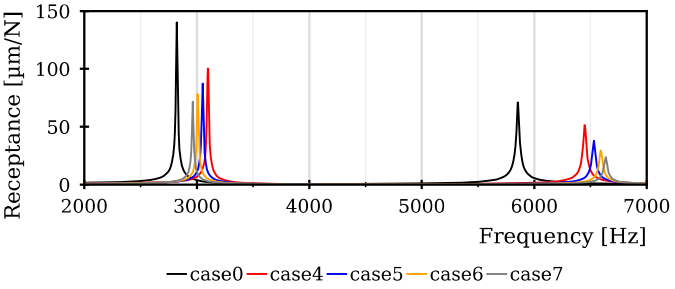

Fig. 6. Effect of increasing thickness at blade hub on IPW FRFs.

By sinusoidally shaping the stock thickness, t, in leading-to-trailing edge direction (case 0 vs. case 8), frequencies of both eigenmodes are shifted to higher values (Fig. 7). The FRF amplitude of the 1st mode is slightly reduced, whereas the 2nd mode shows a slight increase (CL 3 located at trailing edge on suction side is analyzed, adverse trend appears in mid location of the blade).

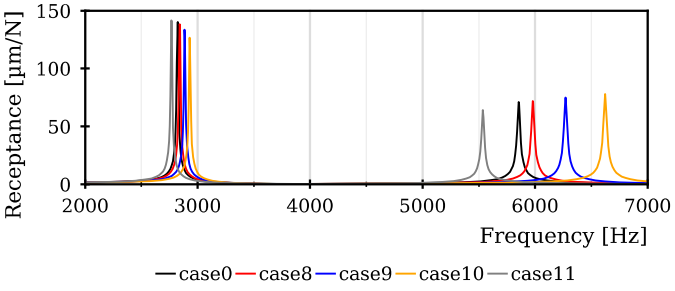

Fig. 7. Effect of sinusoidal stock shape on IPW FRFs.

Increasing the sinusoidal amplitude by 10, 30 and 50 % (case 8 to case 10) leads to a reduction in both the dynamic amplitude and frequency. For a phase shift of 90 deg (case 11), exactly the reverse effect appears.

Such observations are useful to understand the effect of stock shape on the workpiece dynamics. However, considering that the stock thickness, changes the radial depth, a_e, as well, stability analysis is required as discussed in the next section.

4.2. Effect of variable stock on stability diagram

By comparing the IPW FRFs alone, it is difficult to evaluate the process stability of the twelve cases. Through the subsequent stability calculation, the critical depth of cut $a_{p,crit}$ and dynamic magnitude of the dominant mode can be correlated by use of the SLDs, at least for finishing with identical radial depth of cut of 50 µm. However, a correlation between lobes and frequency shift of the eigenmodes is non-trivial especially for a complex freeform surface as the blade geometry and corresponding IPWs during machining process (Fig. 8).

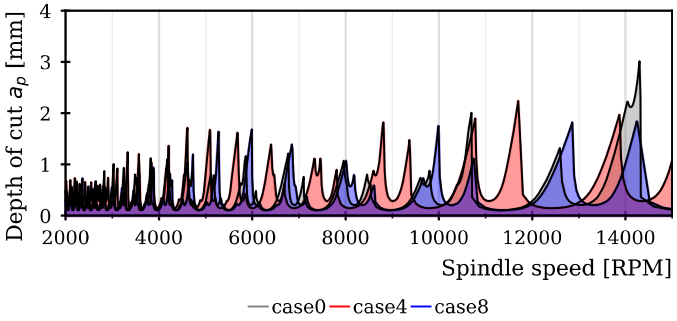

Fig. 8. SLDs of cases 0, 4, and 8 for IPW sfin 6 at CL 3.

Stability KPIs were derived from the calculated stability charts. The critical depth of cut $a_{p,crit}$, the maximum depth of cut $a_{p.max}$ and the area under the stability lobe diagram A_{SLD} (high probability to find stable RPM if high) are used to compare the defined cases in terms of dynamic process stability (Fig. 9).

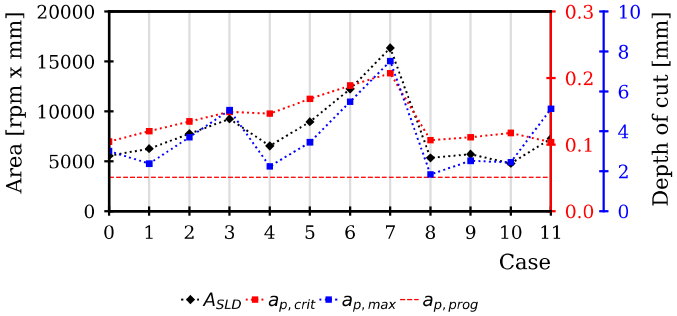

Fig. 9. Stability KPIs of cases 0 to 11 for IPW sfin 6 at CL3.

4.3. Ranking of cases

A novel and practical approach is proposed for comprehensive evaluation of dynamic process stability, whereby the continuously changing workpiece dynamics during the machining process is considered: (i) summarize the stability charts of one CLL by calculating the defined stability KPIs (Section 4.2), (ii) aggregate stability KPIs to one value per case by calculating average and minimum, (iii) rank the cases

by sorting them in descending order for each stability KPI considering average and minimum individually, and (iv) count the occurrence of each case in the top 5 ranks. The case with the most frequent occurrence is evaluated with the highest process stability. Here, the proposed procedure was conducted considering both semi-finishing and finishing. The results are shown in Fig. 10.

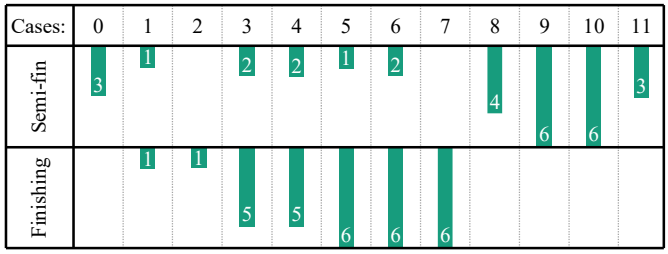

Fig. 10. Ranking of cases with their score (considering minimum), as result of the proposed evaluation methodology.

Comparing the twelve cases, case 6 is evaluated as best case of the “linear” population and case 9 is one of the most advantageous for the “sinusoidal” population. Overall, case 6 is rated as the case with the highest dynamic process stability.

5. Experimental demonstration

In Section 5.1, the experimental setup for machining case 0 (reference), case 6 (linear), and case 9 (sinusoidal) is described. The experimental verification of FEA by comparing the results obtained from experimental modal analysis (EMA) is presented in Section 5.2. Section 5.3 deals with the selection of advantageous spindle speeds at individual cases and altering the spindle speed during merged semi-/finishing process. Finally, the achieved blade surface quality is discussed in Section 5.4.

5.1. Experimental setup

5-axis milling of the blade demonstrator was conducted on a GF Mikron HPM 800U HD vertical machining center. The stock material was clamped with two M8 cylinder head screws on an adapter block with a torque of 40 Nm (Fig. 11).

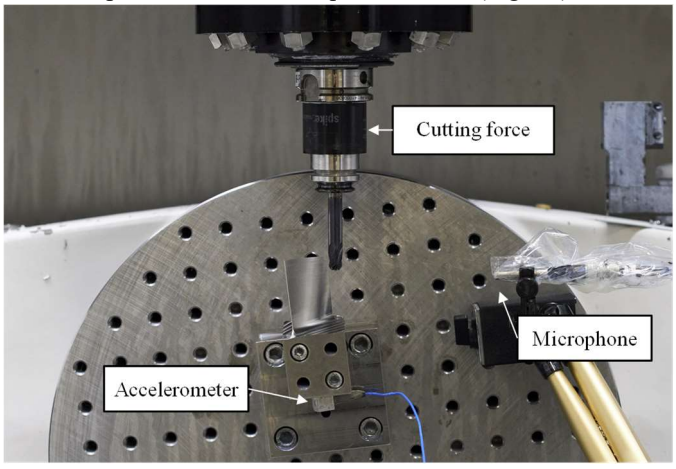

Fig. 11. Blade demonstrator clamped on milling machine

Every operation was executed with another type of milling tool. A ball end mill (BEM) with a diameter of 16 mm was used for pre-roughing (Fig. 2a), BEM with D = 10 mm was used for roughing (Fig. 2b), and a BEM with a diameter of 12 mm, four teeth, and a helix angle of 30 deg was used for the merged semi-/finishing operations (Fig. 2b). The overhang length of the finishing tool was set at 64 mm.

5.2. Experimental verification of FE modal analysis

An experimental modal analysis (EMA) was conducted before the individual finishing operations with the objective to determine the modal parameters of the blade IPWs for all modes in the frequency range of 200 to 12,000 Hz. The measurements were performed with a laser vibrometer (Polytec OFV-5000) and an automatic impulse hammer (PCB 086E80).

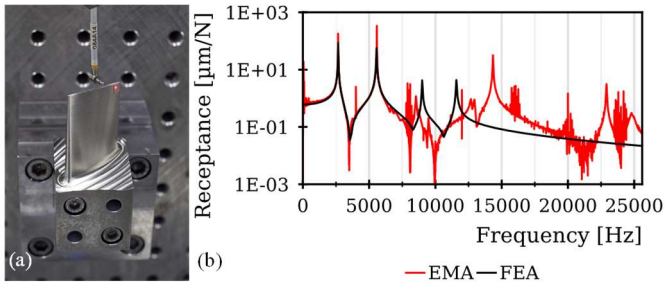

Fig. 12. (a) EMA setup for case 0 “reference” at CL 1, (b) FRF before final merged semi-/finishing operation by EMA (red) and FEA (black).

The eigenfrequencies determined by EMA for the ‘reference’, i.e., case 0, are 2659 Hz and 5580 Hz, which is equal to a relative deviation of 0.19 % and 0.44 % from FE modal analysis. The difference of the dynamic magnitudes for the eigenmodes can be explained by the fact that the damping ratio defined in FEA (0.2 %) deviates from the actual damping ratio (0.09 % and 0.03 %).

5.3. Selection of advantageous spindle speeds

Advantageous spindle speeds were selected individually for merged semi-/finishing operation of each case. A distinction was made between semi-finishing and finishing. For semi-finishing, a lower spindle speed range of 2000 to 5000 RPM was used, for finishing 5000 to 11000 RPM. Starting from the IPW before the final merged semi-/finishing operation, the six IPWs after semi-finishing path number 6, 11, 21, 31, 41, 51 and their corresponding SLDs were used to select advantageous spindle speeds. It was ensured that comparable spindle speeds were used for the three machining cases. Fig. 13 shows exemplary the SLD for finishing of case 0 before final merged semi-/finishing operation used for spindle speed selection.

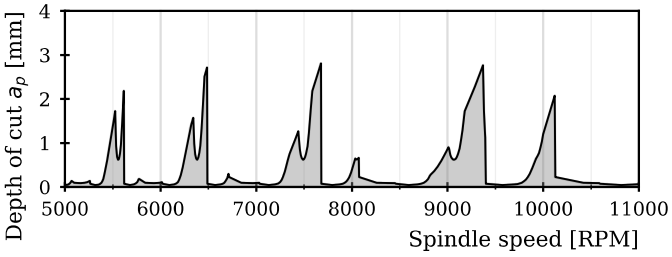

Fig. 13. SLD for finishing of case 0 “reference” before final merged semi-/finishing operation used for spindle speed selection.

5.4. Achieved blade surface quality

Fig. 14 shows the suction side surface of machined case 0 (reference), case 6 (linear group, and case 9 (sinusoidal group). It can be overserved that surface irregularities occurred at top sections along a toolpath of the blade for case 0 (Fig. 14a). Chatter-free surface was achieved for case 6 (Fig. 14b). Vibrations affected the machined surface for case 9 (Fig. 14c) at the top section close to the leading edge and one path slightly further down than for case 0. It can be concluded that the best surface quality was achieved for case 6.

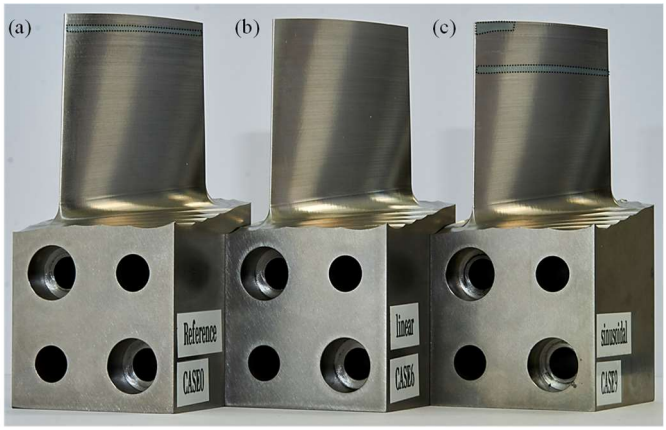

Fig. 14. Suction side surface of machined (a) case 0 “reference”, (b) case 6 “linear”, (c) case 9 “sinusoidal”.

6. Conclusion and outlook

This paper further elaborated the proposed approach by Tunç et al. [13] to select the thickness and shape of the stock for improved stability in 5-axis milling of thin-wall workpieces to an application-oriented use case. Coupled process simulation, which includes material removal, FEA, and stability simulations, was used to analyze the effect of stock shape on process dynamics. The proposed methodology enables the comprehensive evaluation of dynamic process stability, considering the continuously changing workpiece dynamics during the machining process using FE simulations. Based on the varying IPW FRF for selected CLs, spindle speeds were optimized along the toolpath for the merged semi-/finishing processes. Finally, the proposed methodology was successfully demonstrated in machining experiments.

Comprehensive analysis of the acquired process data stands as future work, where data-based evaluation of dynamic process stability of semi-finishing and finishing and its correlation with the simulations should be performed. Furthermore, detailed analysis of the effect of thickness and stock shape on the damping ratio is another issue, which is crucial for the accuracy of FE simulations to predict IPW dynamics and hence chatter stability. Better understanding the relationship between the variable stock shape and damping ratio would enable further improvement in stock shape design.

Acknowledgements

The work has been part of the dynaTWIN Project (E! 115498) funded by the BMBF (Germany), Tübitak (Türkiye), and CDTI (Spain) within the Eurostars (Eureka) program.

References

[1] Quintana, G., Ciurana, J., 2011. Chatter in machining processes: A review. International Journal of Machine Tools and Manufacture 51 (5), 363–376.
[2] Budak, E., Tunç, L., Alan, S., özgüven, H.N., 2012. Prediction of workpiece dynamics and its effects on chatter stability in milling. CIRP Annals 61 (1), 339–342.
[3] Altintas, Y., Stepan, G., Merdol, D., Dombovari, Z., 2008. Chatter stability of milling in frequency and discrete time domain. CIRP Journal of Manufacturing Science and Technology 1 (1), 35–44.
[4] Munoa, J., Beudaert, X., Dombovari, Z., Altintas, Y., Budak, E., Brecher, C., Stepan, G., 2016. Chatter suppression techniques in metal cutting. CIRP Annals 65 (2), 785–808.
[5] Maslo, S., 2022. Simulation of the dynamic vibration behaviour and spindle speed optimization during the milling process of turbomachinery components. Dissertation, 1. Auflage ed., Aachen.
[6] Kolluru, K., Axinte, D., 2013. Coupled interaction of dynamic responses of tool and workpiece in thin wall milling. Journal of Materials Processing Technology 213 (9), 1565–1574.
[7] Thevenot, V., Arnaud, L., Dessein, G., Cazenave–Larroche, G., 2006. Influence of material removal on the dynamic behavior of thin-walled structures in peripheral milling. Machining Science and Technology 10 (3), 275–287.
[8] Maslo, S., Menezes, B., Kienast, P., Ganser, P., Bergs, T., 2020. Improving dynamic process stability in milling of thin-walled workpieces by optimization of spindle speed based on a linear parameter-varying model. Procedia CIRP 93, 850–855.
[9] Petráček, P., Falta, J., Stejskal, M., Šimůnek, A., Kupka, P., Sulitka, M., 2022. Chatter-free milling strategy of a slender Blisk blade via stock distribution optimization and continuous spindle speed change. International Journal of Advanced Manufacturing Technology.
[10] Koike, Y., Matsubara, A., Yamaji, I., 2013. Design method of material removal process for minimizing workpiece displacement at cutting point. CIRP Annals 62 (1), 419–422.
[11] Smith, S., Wilhelm, R., Dutterer, B., Cherukuri, H., Goel, G., 2012. Sacrificial structure preforms for thin part machining. CIRP Annals 61 (1), 379–382.
[12] Tunç, L.T., Ozkirimli, O.M., Budak, E., 2016. Machining strategy development and parameter selection in 5-axis milling based on process simulations. Int J Adv Manuf Technol 85 (5-8), 1483–1500.
[13] Tunç, L.T., Zatarain, M., 2019. Stability optimal selection of stock shape and tool axis in finishing of thin-wall parts. CIRP Annals 68 (1), 401–404.
[14] Rudel, V., Kienast, P., Vinogradov, G., Ganser, P., Bergs, T., 2022. Cloud-based process design in a digital twin framework with integrated and coupled technology models for blisk milling. Front. Manuf. Technol. 2.
[15] Altintaş, Y., Budak, E., 1995. Analytical Prediction of Stability Lobes in Milling. CIRP Annals 44 (1), 357–362.